RESEARCH ARTICLE Agricultural Science Digest, Volume 45 Issue 6: 940-950 (December 2025)

Biologically Derived Nanohydroxyapatite: A Comparative Analysis with a Commercial Counterpart

Arati Patil[1], Nagesh Aloorkar[1], Anand Kakde[2], Mangesh Mapari[2], Sandip Sapkal[2], Gauri Laddhad[3]

10.18805/ag.D-6312

ABSTRACT

Background: In the present paper, Nano-Hydroxyapatite (n-HAp) is synthesized from Indian Hen (Busra breed) and Hybrid Hen eggshell waste using chemical precipitation methods. The principal objectives of this research are to synthesize natural HAp from eggshell waste and comparing with commercial available Hydroxyapatite (HAp) as reference sample (NnanoXIM-Hap-202).

Methods: Analytical methods were used to characterize n-HAp and HAp including Fourier Transform Infrared Spectroscopy (FTIR), X-Ray Diffraction (XRD), Scanning Electron Microscopy (SEM), Energy Dispersive Spectroscopy (EDS), Differential Scanning Calorimetry (DSC) and Thermogravimetry-Differential Thermal Analysis (TG-DTA). Calcinations of eggshell waste at 850 to 900°C yielded HAp with a calcium/phosphorus ratio of 1.71 to 1.75.

Result: A comparative analysis with a reference sample (commercially available HAp) revealed that the synthesized HAp exhibited similar structural and chemical properties, with slight variations in their morphological and thermal characteristics.

Key words: Bone graft, Calcium-phosphorus ratio, Eggs shell, Hydroxyapatite, Nanoparticles.

INTRODUCTION

In today's clinical practices, treating bone abnormalities, including arthrodesis (fusion), spondylodesis, bone excision or bone cutting and gelation under bone conditions is difficult. Bone graft techniques, including demineralization and deproteinization (xenograft), autogenous bone grafts (allografts) and bone substitution (autografts), are commonly used in clinical practice to repair damaged tissue. However, it is not practical because of the lack of graft material and the possibility of immunological refusal (Meskinfam *et al*., 2018). Undoubtedly, the increasing need for artificial bone transplantation is a result of longer life expectancies. The material used for grafting should meet crucial physiological and biomechanical criteria, including interconnected porosity with suitable mechanical stiffness, bioactivity, biocompatibility and biodegradability. Ninety per cent of the minerals in human bone are calcium phosphates, especially HAp, with the other 10% to 20% being water, inorganic salts, collagen fibers and proteins (Taz *et al*., 2019; Jalageri *et al*., 2022). As a consequence, HAp has been recognized as a bone tissue matrix material. The collagen-hydroxyapatite composite serves as a synthetic bone graft, replicating the properties of natural bone and offering excellent osteoconductivity for enhanced bone regeneration and it is proven by one study when compared to intramedullary pins alone, hydroxyapatite-collagen composite with autologus bone marrow concentrate speeds up the healing of fractures in dogs (Jain *et al*., 2023).

Hydroxyapatite implants are widespread in orthopedics, dentistry and other fields. spondylodesis therapy, synthetic bone grafts for bone-cutting procedures. Calcium and phosphate are obtained from a variety of chemical precursors to produce HAp in large quantities (Venkatesan *et al*., 2016; Prabakaran *et al*., 2021). Despite this, the application of hazardous chemicals and surfactants could affect biocompatibility, which could interfere with the ability of *in vivo* cells to regain their properties (Fihri *et al*., 2017). In addition, artificial HAp implants are devoid of rare ingredients such as Mg (magnesium) and trace amounts of Cu (copper), Fe (metal), Mg (manganese), Zn (zinc) and K (potassium) salts are crucial for the construction of new bone cells. In this context, choosing a calcium source for ceramics in the biomaterial formation process is fundamental since it has an immense effect on the purity and stoichiometry of the final product.

[1]Department of Pharmaceutics, Satara College of Pharmacy, Satara-415 004, Maharashtra, India.
[2]Department of Pharmaceutics, Laddhad College of Pharmacy, Yelgaon Buldana-443 001, Maharashtra, India.
[3]Dr Balasaheb Vikhe Patil Rular Medical College, Loni-413 736. Maharashtra, India.

Corresponding Author: Arati Patil, Department of Pharmaceutics, Satara College of Pharmacy, Satara-415 004, Maharashtra, India. Email: arati.patil1690@gmail.com
ORCIDs: https://orcid.org/0009-0003-4920-8064, https://orcid.org/0000-0001-8681-757X, https://orcid.org/0009-0005-1884-2948, https://orcid.org/0000-0002-7089-9424, https://orcid.org/0000-0001-5626-8469, https://orcid.org/0009-0006-9714-2559

How to cite this article: Patil, A., Aloorkar, N., Kakde, A., Mapari, M., Sapkal, S. and Laddhad, G. (2025). Biologically Derived Nanohydroxyapatite: A Comparative Analysis with a Commercial Counterpart. *Agricultural Science Digest.* **45(6):** 940-950. doi: 10.18805/ag.D-6312.

Submitted: 14-02-2025 **Accepted:** 14-04-2025 **Online:** 27-06-2025

Since calcium carbonate or $CaCO_3$ makes up 95-97% of natural sources such as chicken eggshells, they can be used as a source of raw calcium materials. When in contact with human tissues, these biogenic sources provide swift biomineralization (Castro *et al*., 2022). The implants are nontoxic and maintain MG 63 osteoblast-like cells, according to the results of a study on the *via*bility of HAp cells made from eggshells (Krishna *et al*., 2007).

India produces the third most eggs worldwide, behind the U.S.A. and China, on the basis of an investigation published by the United Nations Food and Agriculture Organization. In the fiscal year of 2018-2019, the nation produced 92 billion eggs. In 2019-2020, the poultry business in India increased at an approximate yearly growth rate of 8% and over the next five years, it is projected to rise by 12%. Because of the microbiological activity of the shell membrane, shells obtained from hen eggs are regarded as worthless biowaste material and their amassing poses a major environmental risk. As a result, the use of shells of eggs to produce biomaterials on a massive scale, such as HAp is essential (Kumar *et al*., 2023).

The mineral impurities in the shells of some Indian chicken breeds are ten times greater than those in the shells of boiler (hybrid) eggs (Lordelo *et al*., 2020). In light of this, we used Indian native chicken shells from the hilly parts of Maharashtra, India, for the current study. Rare minerals such as selenium (Se), magnesium (Mg), fluoride (F) and strontium (Sr) are found in these calcium-rich shells and help to generate interfacial bone tissue. Strontium-substituted hydroxyapatite (SrHAp) was used to assess how strontium affects osteoblast differentiation. Strontium promotes the development of osteoblasts into osteocytes (Stipniece *et al*., 2020). Utilizing biowaste like eggshells in sustainable materials synthesis holds significant promise. Eggshells provide a readily available, renewable resource for creating valuable products, thereby reducing our reliance on mined materials. This approach also addresses environmental concerns related to waste disposal. Furthermore, eggshell-derived materials exhibit biocompatible properties, making them suitable for biomedical applications, particularly as a source of calcium for bone-related treatments (Abdulrahman *et al*., 2014).

Biologically sourced n-HAp emerges as a viable substitute for commercially produced hydroxyapatite in numerous biomedical applications, with a particular emphasis on bone regeneration. Empirical evidence suggests that minimizing the particle size of HAp to the nanometer scale significantly enhances its osteoconductive properties (Vani *et al*., 2021). Moreover, the integration of inorganic materials has been shown to augment interactions between osteoblast cells and the material, thereby promoting bone formation (Vani *et al*., 2021). Notably, multi-ion doped nano-hydroxyapatite coatings applied to titanium implants have yielded outstanding functional results in the treatment of long bone fractures in canine models, characterized by early limb utilization and an absence of post-operative complications (Vani *et al*., 2021). Additionally, the application of autologous bone marrow concentrate in combination with hydroxyapatite-collagen has been associated with early weight-bearing and successful fracture union in dogs (Jain *et al*., 2023).

In this investigation, HAp was synthesized from the eggshells of Indian hen eggs and the hybrid hen egg shell and the product was compared with the reference sample (NnanoXIM-Hap-202).

MATERIALS AND METHODS

Material

Indian hen eggs (Busra breed) were purchased from a local market, Diammonium Hydrogen Phosphate (D.A.P.) Pallav Chemicals and Solvents Pvt Ltd. Mumbai, India. NnanoXIM-Hap-202 as a gift sample for reference purposes was obtained from Fluidinova,S. A Maia Portugal and Double Distil Water (D.D.W).

Method

Various methodologies are employed in the synthesis of hydroxyapatite (HAP)-like products, including the precipitation technique, sol-gel approach, hydrothermal technique or wet method, multiple emulsions, biomimetic deposition and electrodeposition. Among these, the precipitation technique is particularly valued for its simplicity and scalability.

In the precipitation method, calcium oxide (CaO) is obtained from the egg shells of Indian hen egg (IE) and hybrid hen egg (HE), which is followed by a confirmatory test of CaO after the test of Hap synthesis as a precipitated product of CaO and D.A.P. reactions. Fig 1 shows the process's visual portrayal. The study was conducted in Pharmaceutical Department of Satara College of pharmacy Satara, Maharashtra and study conducted from February 2022 to January 2025.

1) Boiling water was used to clean the egg shells. After that, the samples were dried at 25°C in an oven.
1) The dried egg shells were crushed *via* a mortar and pestle.
2) For the formation of CaO powder, crushed egg shells were sintered for four hours at 850-900°C.
3) Different concentrations of diammonium hydrogen phosphate (D.A.P.) solution, as shown in Table 1, were used to treat the calcium oxide solution with a magnetic stirrer for 1 hr. at 100°C
4) After one hour, the precipitate of hydroxyapatite was prepared.
5) The resulting HAp precipitate was filtered through Whatman filter paper and dried for four to five hours at 100°C in an oven.

Physicochemical characterization

The synthesis of HAp was confirmed *via* the conventional FTIR spectroscopic technique. XRD was used to identify the phases of the crystalline material. SEM was used to study the morphology of the HAp particles, including their shape, size and surface texture and EDS was used to determine the weight and atomic percentages of all the

elements in the HAp, which can be used to calculate the calcium-to-phosphate ratio. To examine the thermal stability and thermal response of the synthesized HAp powders, DSC, TG and DTA were performed.

Characterization of HAp

FTIR

HAp was investigated *via* FTIR using a KBr pellet. The sample preparation involved grinding HAp into a fine powder, mixing it with KBr powder and compressing the mixture into a thin pellet. The pellet was then inserted into a SHIMADZU IR Prestige 21 spectrometer (SHIMADZU Cooperation, Japan) and the 4000-400 cm^{-1} wave number range was used to record the FTIR spectra.

XRD

The obtained HAp powder was structurally characterized *via* XRD analysis. The XRD pattern was recorded *via* a Rigaku Ultima (Version-IV) diffractometer (Rigaku, Japan) with Cu Kα radiation (λ = 1.5406 Å) at 40 KeV and 40 mA. The XRD patterns of the samples were compared with the reference sample diffraction data.

SEM and EDS

SEM

SEM was used to analyze the surface structure and properties of the HAp powder. A [FEI Nova NanoSEM 450] SEM instrument operating at 1.0 nm at 15 kV, 1.4 nm at 1 kV and 1.8 nm at 3 kV and 30 Pa was used. With the use of a sputter coater, a small layer of gold was applied to the samples to improve conductivity and stop charging.

EDS

EDS was used to verify the fundamental constitution of the HAp powder. The samples were evaluated at 123 eV with Mn Ká radiation and 45 eV with C Kα radiation *via* an EDS detector [Bruker XFlash 6I30], with element detection ranges ranging from 4 Be to 95 Am. FESEM: XT microscope Control EDS: Espirit 1.9 software was used to find and investigate the EDS spectra.

DTA-TG and DSC

The thermal properties of Standard Hap, IE 1 and HE1 were investigated *via* DTA-TG and DSC techniques. DTA and TG analysis were performed *via* Thermogravimetric Analyzers model number SDT 650 (Waters) and Trios software. The sample was heated from room temperature to 1200°C/min at a rate of 5°C/min. DSC analysis was performed *via* a DSC 1 star system (Mettler Toledo) and samples were prepared from room temperature to 300°C at a heating rate of 10°C/min.

RESULTS AND DISCUSSION

FTIR

The molecular structures of the materials were investigated *via* Fourier transform infrared (FTIR) spectroscopy. The FTIR spectrum of HAp typically exhibits several characteristic peaks. The broad peak at 3500-3600 cm^{-1} indicates the presence of hydroxyl ions due to hydroxyl (-OH) stretching. Strong peaks between 1000-1100 cm^{-1} and 500-600 cm^{-1} correspond to the symmetric and asymmetric stretching of phosphate (PO4) groups. Additionally, the peaks at 1400-1500 cm^{-1} and 800-900 cm^{-1} indicate the presence of carbonate (CO_3) ions, if present. Furthermore, the peaks between 600 and 800 cm^{-1} are attributed to the bending vibrations of phosphate and hydroxyl groups, (Venkatesh *et al*., 2002). Whereas the peaks below 500 cm^{-1} are associated with the lattice vibrations of the HAp crystal structure (Fathi *et al*., 2007).

In HAp, carbonate groups (if present) exhibit a frequency range of 1400-1500 cm-1[3]. This phenomenon is observed when eggshell calcinations are inadequate. $CaCO_3$ was detected in samples IE2, IE3, HE2 and HE3, with corresponding frequencies of 1408.75, 1464 and 1415.49 cm^{-1}, respectively. Conversely, the presence of phosphate

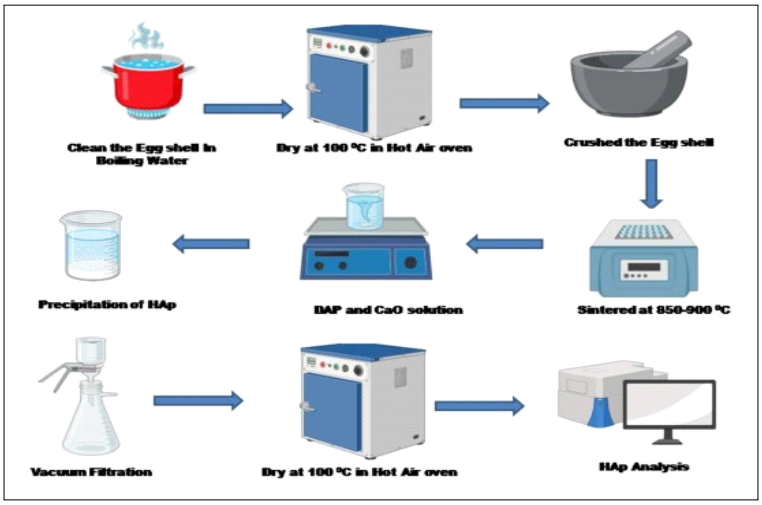


Fig 1: Chart representation of the HAp synthesis process.

and hydroxyl groups is denoted by frequencies of 3500-3600 cm^{-1} and 1000-1100 cm^{-1}, respectively. All the prepared samples displayed distinctive peaks at 3652.30, 3639.02, 3640.87, 3641.10, 3517.52, 3647.42 and 3650.74 cm^{-1}, attributed to phosphate stretching and at 1024.83, 1028.84, 1032.49, 1027.98, 1027.87, 1030.57 and 1031.27 cm^{-1}, corresponding to hydroxyl stretching. The peaks within the frequency range of 500–600 cm^{-1} indicate the formation of the HAp crystal lattice structure (Venkatesan *et al*., 2016). (Table 2 and Fig 2) Consequently, the FTIR analysis of the

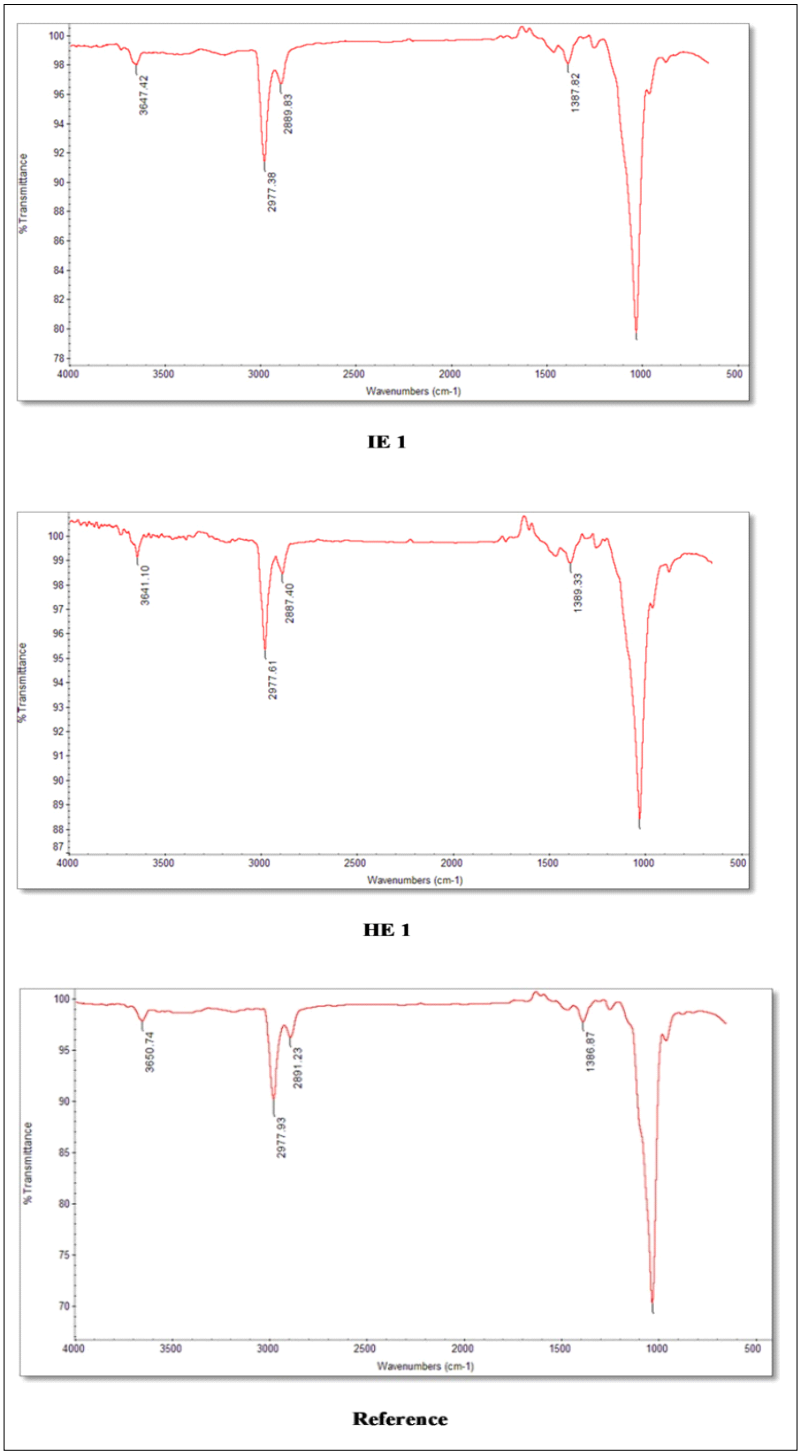


Fig 2: FTIR spectrum of the IE 1, HE1 and reference sample.

HAp powder samples revealed that samples IE1 and HE1 yielded appropriate results, whereas the other samples exhibited some degree of deviation.

XRD

Fig 3 displays the XRD pattern of the calcined HAp sample. High crystallinity is indicated by the appearance of distinct, sharp peaks in the diffraction pattern. The maximum intensity well-resolved characteristic peak is observed at 2θ = 31.74° (IE) and 31.70° (HE), which corresponds to the pure HAp data and the standard HAp sample (JCPDS# 72-1243). The synthesis of stoichiometric HAp in the apatite phase was confirmed by the existence of this distinctive HAp peak in addition to other peaks. Every diffraction peak is in good agreement with the standard apatite HAp diffraction data.

SEM

The SEM micrographs of the reference HAp powder revealed a uniform morphology with regularly shaped particles and the average particle size ranged between 825 nm and 9.1 µm, as shown in Fig 4. The particles exhibited a rough surface texture, indicating a high surface area with a porous nature. The particles of IE-1 and HE-1 have rough surface textures, irregular shapes, and average sizes between 16.9 and 37.77 nm and between 26.9 and 37.77 nm, respectively.

Table 1: Batches of IE and HE with different concentrations of D.A.P and D.D.W.

Compound	Cao(g)	DDM (ml)	D.A.P(g)	D.D.W (ml)
IE 1	4	240	7.5	95
IE 2	4	240	3.75	48
IE 3	4	240	1.875	24
HE 1	4	240	7.5	95
HE 2	4	240	3.75	48
HE 3	4	240	1.875	24

EDS

The EDS spectra of the reference, IE-1 and HE-1 HAp powders presented calcium (Ca), phosphorus (P) and oxygen (O) peaks, confirming the composition of HAp presented in Fig 5. Compared with those of the reference samples, the atomic percentages of Ca, P and O and the Ca/P atomic ratios of the IE-1 and HE-1 samples were found to be satisfactory in Table 3. The elemental map images show the distributions of Ca, P and O within the sample and the reference images are shown in Fig 6. X-ray map images show the distribution of X-rays emitted by the sample, which represent the presence of specific elements within the synthetic sample and reference HAp sample, as presented in Fig 7.

Thermal analysis

TG and DTA

The weight losses of 0.032%, 0.0711% and 0.054% in the temperature range of room temperature to 1200°C are shown by the TG and DTA curves in Fig 8. This loss is caused by the breakdown of organic contaminants and the loss of adsorbed water.

Table 2: FTIR interpretation data.

Frequencies Required	IE1	IE2	IE3	HE1	HE2	HE3	Reference
3500-3600	3647.42	3639.02	3640.87	3641.10	3517.52	3639.02	3650.74
1400-1500	-	1408.75	1400.00	-	1415.49	1405.85	-
1000-1100	1100.87	1028.84	1032.49	1027.98	1083.83	1030.57	1031.27
800-900	-	872.631	875.760	-	873.596	872.639	-

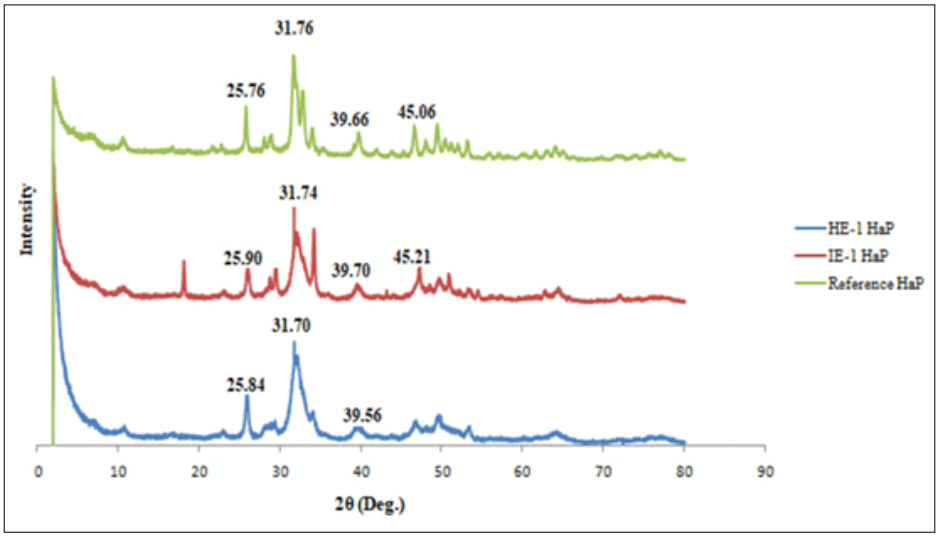


Fig 3: XRD patterns of HE-1, IE-1 and Reference HAp.

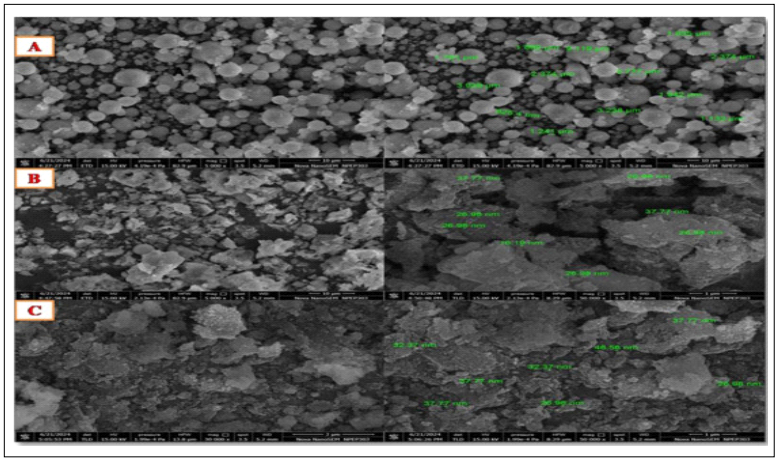


Fig 4: SEM micrographs of A) reference samples B) IE-1 and C) HE-1.

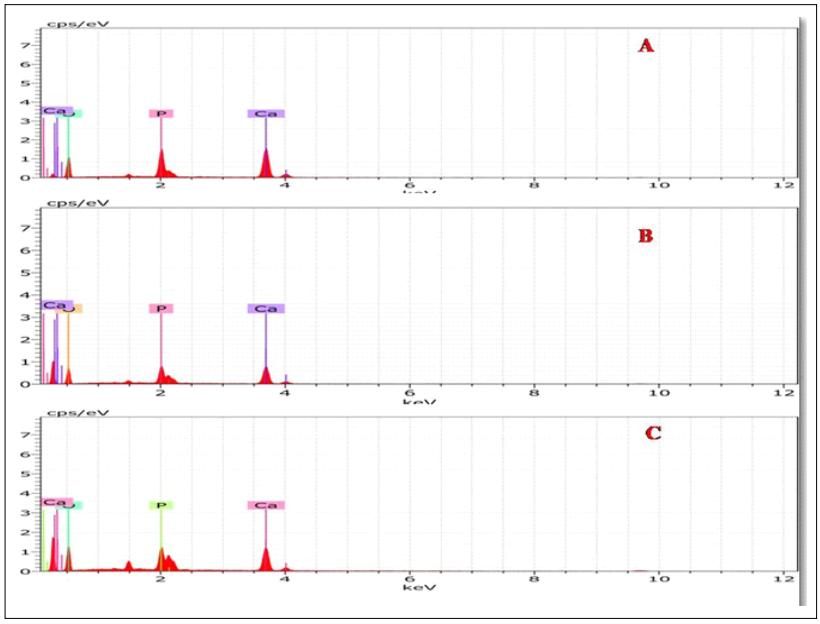


Fig 5: EDS spectra of A) reference sample B) IE-1 and C) HE-1, which represent the elemental composition of Ca, P and oxygen O with the corresponding Kα peaks.

Table 3: Estimation of the atomic percentage and Ca/P ratio *via* EDS.

Sample	Element	Atomic percentage	Ca/P ratio
Reference HAp powder	O	67.72	1.71
	Ca	22.63	
	P	10.26	
	Total	100	
IE-1 HAp powder	O	69.73	1.74
	Ca	20.98	
	P	9.29	
	Total	100	
HE-1 HAp powder	O	72.15	1.72
	Ca	19.23	
	P	8.63	
	Total	100	

DSC

The DSC curves for the three HAp samples (A, B and C) are shown in Fig 9. Exothermic peaks are observed in the DSC curves at 90.20°C, 91.16°C and 99.59°C. Curves indicate the occurrence of exothermic reactions, such as crystallization or decomposition, in the HAp samples.

The results of this study provide a comprehensive evaluation of the potential of biologically derived nanohydroxyapatite (n-HAp) synthesized from Indian hen and hybrid hen eggshell waste as a viable alternative to commercially available hydroxyapatite (HAp) (Kumar *et al*., 2010) (Prakash *et al*., 2024). The successful synthesis of n-HAp from eggshells was confirmed through multiple characterization techniques. Fourier Transform Infrared (FTIR) spectroscopy revealed distinct peaks corresponding to hydroxyl and phosphate groups, characteristic of hydroxyapatite. Minor peaks attributed to residual carbonate ions in some batches (*e.g.*, IE2, IE3, HE2 and HE3) suggest incomplete calcination, emphasizing the importance of precise control over the synthesis conditions to eliminate impurities (Francis *et al*., 2024) (George *et al*., 2020).

The presence of essential functional groups and the absence of significant contamination validate the chemical suitability of the synthesized n-HAp for biomedical applications. X-ray Diffraction (XRD) analysis demonstrated high crystallinity in the synthesized samples, with diffraction patterns closely matching those of the commercial reference sample (NnanoXIM-Hap-202) (Fitriyana *et al*., 2024). The primary peak at 2θ = ~31.7° aligns well with the apatite phase, confirming the successful formation of stoichiometric hydroxyapatite. High crystallinity is crucial for the mechanical stability and bioactivity of HAp, suggesting that the synthesized material meets the structural requirements for orthopedic and dental applications. Scanning Electron Microscopy (SEM) revealed significant

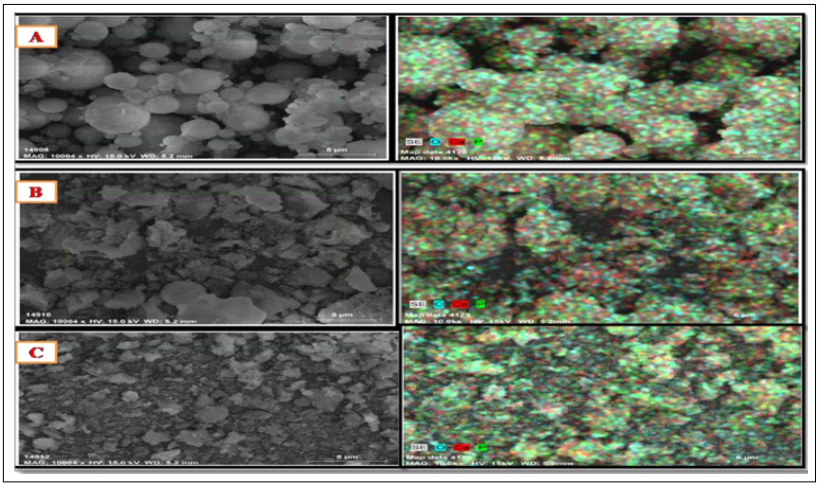


Fig 6: EDS elemental map images of A) reference sample B) IE-1 and C) HE-1.

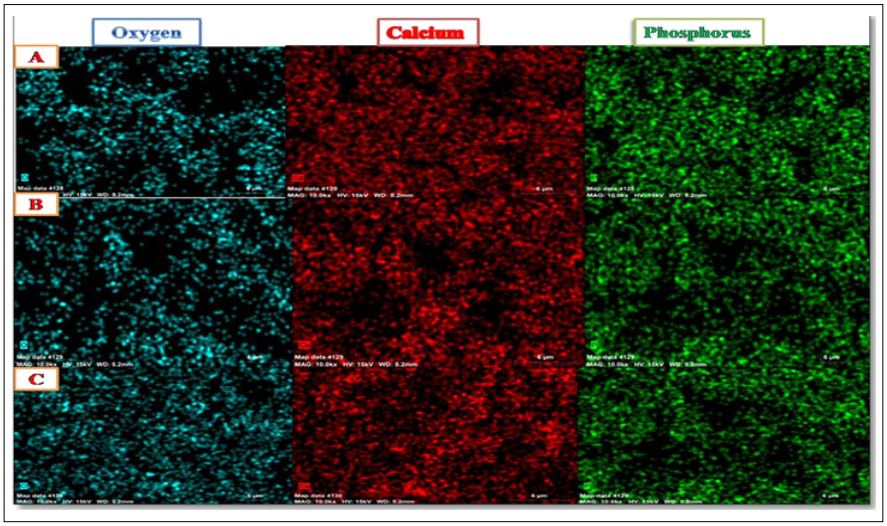


Fig 7: EDS X-ray map images of A) reference sample B) IE-1 and C) HE-1.

differences in the morphology of synthesized and commercial HAp (Mondal *et al*., 2023). While the reference sample exhibited uniform, spherical particles with smoother surfaces, the n-HAp samples displayed rougher surfaces and irregular shapes.

The particle size of the synthesized HAp was in the nanoscale range (~16.9 to 37.77 nm), smaller than the commercial counterpart (~825 nm to 9.1 µm), indicating enhanced surface area. The nanoscale size and increased surface roughness of synthesized HAp are advantageous

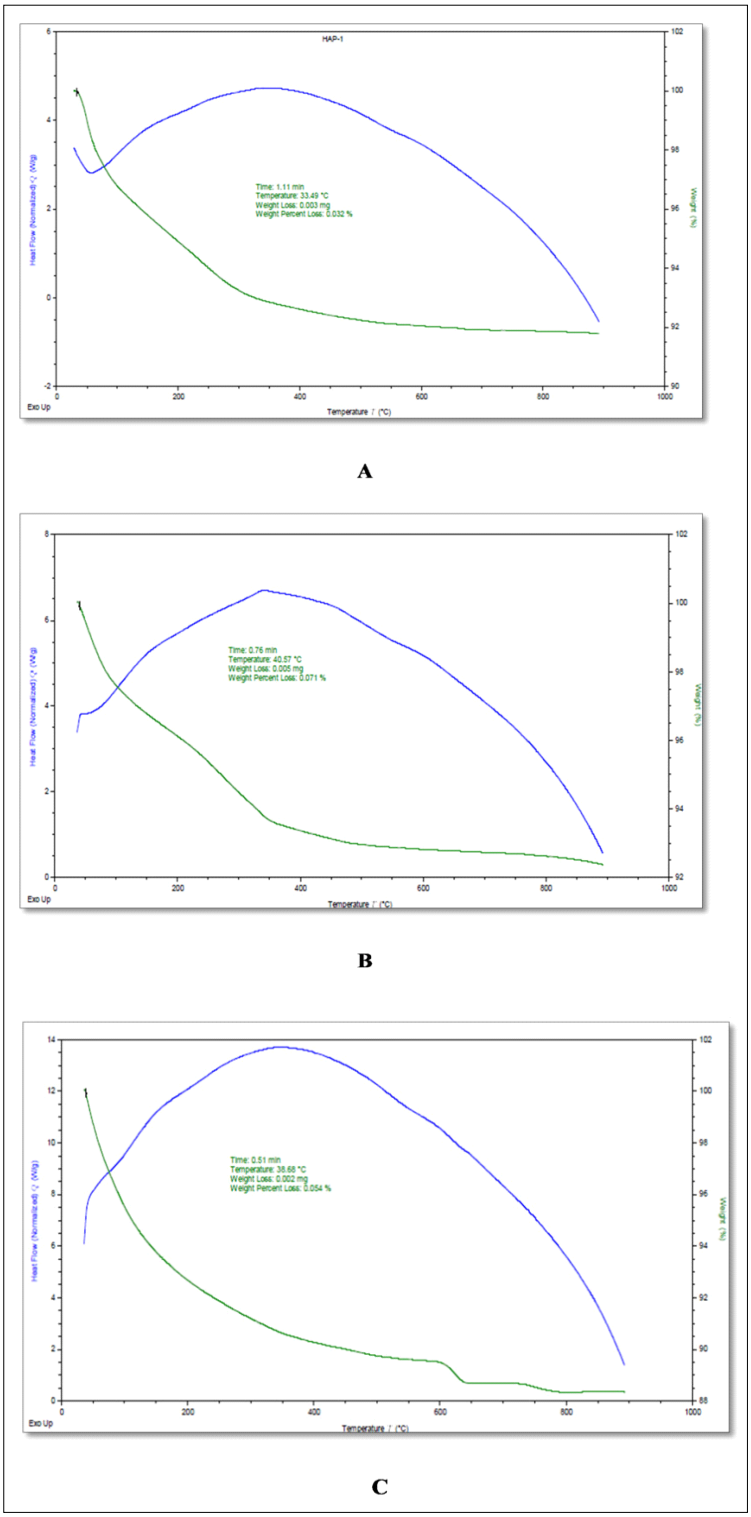


Fig 8: TG and DTA graphs of A) reference sample B) IE-1 and C) HE-1.

for cellular interactions, bone integration and bioactivity, despite minor deviations in morphology from the commercial sample (Damiri *et al*., 2024). Energy Dispersive Spectroscopy (EDS) confirmed the presence of calcium, phosphorus and oxygen in the synthesized n-HAp, with a Ca/P ratio ranging from 1.71 to 1.75-closely matching the ideal ratio for biological HAp. This ratio ensures optimal biocompatibility and mechanical properties. The close match in elemental composition and Ca/P ratio underscores the potential of eggshell derived HAp as a functional material for bone regeneration. Thermal analysis (TG-DTA and DSC) indicated excellent thermal stability of the synthesized n-HAp, comparable to the commercial reference. Weight loss profiles due to water and organic material decomposition were minimal, demonstrating the material's resilience under physiological conditions. Thermal stability supports the application of synthesized HAp in high-temperature processes such as sintering for implant fabrication. The utilization of eggshell waste addresses two major challenges: reducing environmental

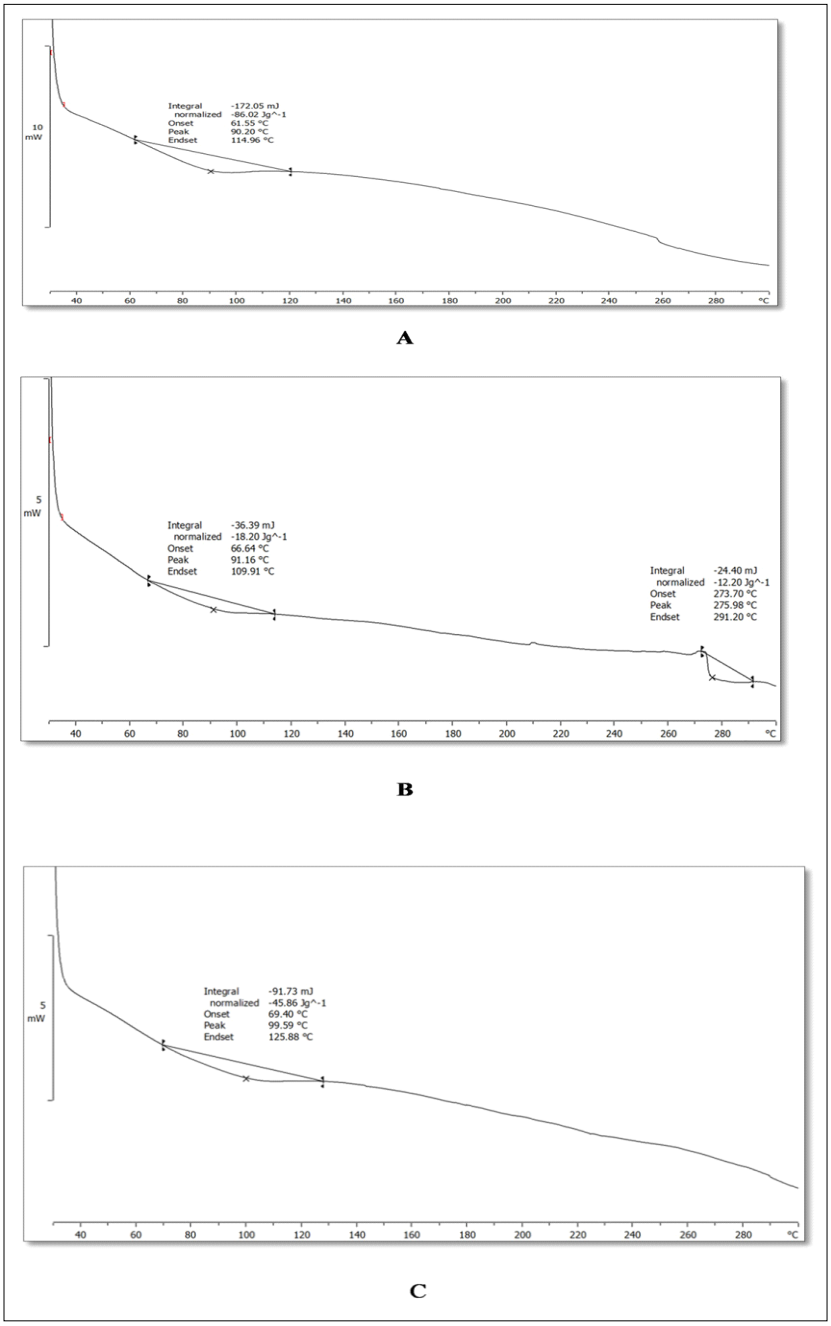


Fig 9: DSC graphs of A) reference sample B) IE-1 and C) HE-1.

impact from biowaste and providing a cost-effective raw material for HAp synthesis (Ammar *et al*., 2023).

The study's findings highlight the potential of using a readily available, renewable resource to meet the growing demand for biocompatible materials in healthcare. Although the synthesized HAp showed slight morphological and thermal deviations from the commercial reference, the structural and chemical similarities suggest that it can serve as a comparable alternative in biomedical applications. The minor differences may even provide unique advantages, such as enhanced cell adhesion due to surface roughness. These results position eggshell-derived n-HAp as a promising candidate for replacing or complementing commercially produced HAp in applications such as bone grafts, implants and tissue engineering scaffolds. To build on the current findings, future research should prioritize optimizing the synthesis conditions to minimize residual impurities, ensuring the purity and consistency of the synthesized hydroxyapatite (HAp).

Investigating the *in vitro* and *in vivo* biocompatibility and bioactivity of the material is crucial to validate its performance in biological systems and establish its suitability for clinical applications. Additionally, incorporating trace elements such as magnesium and zinc could enhance the osteoconductivity and overall functionality of the HAp, mimicking the natural composition of bone tissue. Exploring these enhancements could further improve the material's efficacy in promoting bone regeneration and integration. Scaling up the production process for industrial and clinical use is another essential step, which will involve developing cost-effective, efficient and environmentally friendly manufacturing techniques. This will not only ensure the widespread availability of eggshell-derived HAp but also position it as a sustainable and competitive alternative in the biomedical market. Furthermore, advanced studies into the long-term stability and mechanical properties of the material under physiological conditions are needed to confirm its durability for orthopedic and dental applications. By addressing these areas, future research can maximize the potential of eggshell-derived nanohydroxyapatite and expand its role in regenerative medicine (Kumar *et al*., 2023) (George *et al*., 2020) (Ammar *et al*., 2023).

CONCLUSION

This study successfully synthesized nanohydroxyapatite (n-HAp) from Indian hen and hybrid hen eggshell waste using a sustainable and scalable chemical precipitation method. The synthesized n-HAp was characterized using advanced analytical techniques such as FTIR, XRD, SEM, EDS, DSC and TG-DTA. These analyses confirmed the structural, chemical and morphological properties of the synthesized n-HAp and revealed its close resemblance to commercially available hydroxyapatite, with minor differences in thermal and morphological attributes. The calcium/phosphorus ratio and crystalline characteristics of the synthesized n-HAp demonstrated its suitability for biomedical applications. The findings underscore the potential of utilizing eggshell waste as an eco-friendly and cost-effective source for hydroxyapatite production. This approach not only addresses environmental concerns associated with eggshell disposal, but also offers significant promise in developing biocompatible materials for applications in bone grafts, implants and tissue engineering. Future research could explore optimization of the synthesis process and clinical validations to further establish the synthesized n-HAp as a viable alternative to commercial hydroxyapatite in biomedical applications.

ACKNOWLEDGEMENT

The authors would like to thank Central Instrumentation facility, Savitribai Phule Pune University, Pune for providing Lab facility and support during research work.

Disclaimers

The views and conclusions expressed in this article are solely those of the authors and do not necessarily represent the views of their affiliated institutions. The authors are responsible for the accuracy and completeness of the information provided, but do not accept any liability for any direct or indirect losses resulting from the use of this content.

Conflict of interest

The authors declare that there are no conflicts of interest regarding the publication of this article. No funding or sponsorship influenced the design of the study, data collection, analysis, decision to publish, or preparation of the manuscript.

REFERENCES

Abdulrahman, I., Tijani, H.I,, Mohammed, B.A., Saidu, H., Yusuf, H., Jibrin, M.N. *et al.* (2014). From garbage to biomaterials: An overview on egg shell based hydroxyapatite. *Journal of Materials*. pp 1-6. https://doi.org/10.1155/2014/802467.

Ammar, M., Ashraf, S., Baltrusaitis, J. (2023). Nutrient-doped Hydroxyapatite: Structure, synthesis and properties. *Ceramics*. **6:** 1799-1825. doi.org/10.3390/ceramics6030110.

Castro, F.L.S., Chai, L., Arango, J., Owens, C.M,, Smith, P.A., Reichelt, S. *et al.* (2022). Poultry industry paradigms: Connecting the dots. *The Journal of Applied Poultry Research.* **32:** 100310. doi.org/10.1016/j.japr.2022.100310.

Damiri, F., Fatimi, A., Musuc, A.M., Santos, A.C., Paszkiewicz, S., Idumah, C.I., Singh, S., Varma, R.S., Berrada, M. (2024). Nano-hydroxyapatite (nHAp) scaffolds for bone regeneration: Preparation, characterization and biological applications. *Journal of Drug Delivery Science and Technology*. **18:** 105601 doi.org/10.1016/j.jddst.2024.105601.

Fathi, M.H., Hanifi, A., Mortazavi, V. (2007). Preparation and bioactivity evaluation of bone-like hydroxyapatite nanopowder. *Journal of Materials Processing Technology*. **202:** 536-542. doi.org/10.1016/j.jmatprotec.2007.10.004.

Fihri, A., Len, C., Varma, R.S., Solhy, A. (2017). Hydroxyapatite: A review of syntheses, structure and applications in heterogeneous catalysis. *Coordination Chemistry Reviews*. **347:** 48-76. doi.org/10.1016/j.ccr.2017.06.009.

Fitriyana, D.F., Ismail, R., Bayuseno, A.P., Widodo, R.D., Rusiyanto, R., Anis, S., Siregar, J.P., Cionita, T. (2024). Synthesis of hydroxyapatite from biological sources prepared by the microwave irradiation method: A review. *Engineering Letters.* **32:** 10.

Francis, A.A. (2024). Ecologic and economic motives for transforming calcium-based food wastes into sustainable value-added products: A review. *Environmental Science and Pollution Research.* **32:** 428-451. doi.org/10.1007/s11356-024-35649-w.

George, S., Mehta, D., Saharan, V.K. (2020). Application of hydroxyapatite and its modified forms as adsorbents for water defluoridation: An insight into process synthesis. *Reviews in Chemical Engineering.* **36:** 369-400. doi.org/10.1515/revce-2017-0101.

Jain, R., Shukla, B.P., Shukla, S., Chhabra, D., Karmore, S.K. and Shrivastava, N. (2023). Evaluation of autologous bone marrow concentrate along with hydroxyapatite-collagen for management of long bone fracture in canines. *Indian Journal of Animal Research.* **57(12):** 1678-1685. doi: 10.18805/IJAR.B-4519.

Jalageri, M.B., Kumar, G.C.M. (2022). Hydroxyapatite reinforced polyvinyl Alcohol/Polyvinyl pyrrolidone based hydrogel for cartilage replacement. *Gels.* **8:** 555.

Krishna, D.S.R., Siddharthan, A., Seshadri, S.K., Kumar, T.S.S. (2007). A novel route for synthesis of nanocrystalline hydroxyapatite from eggshell waste. *Journal of Materials Science Materials in Medicine.* **18:** 1735-1743. doi.org/10.1007/s10856-007-3069-7.

Kumar, B.Y.S., Kumar, G.C.M., Shahapurkar, K., Tirth, V., Algahtani, A., Al-Mughanam, T. *et al.* (2023). Processing and characterization of egg shell derived nano-hydroxyapatite synthetic bone for Orthopaedic and Arthroscopy implants and substitutes in dentistry. *Journal of Mechanical Behavior of Biomedical Materials.* **7:** 105963. doi.org/10.1016/j.jmbbm.2023.105963.

Kumar, G.S., Girija, E.K., Thamizhavel, A., Yokogawa, Y. and Kalkura, S.N. (2010). Synthesis and characterization of bioactive hydroxyapatite-calcite nanocomposite for biomedical applications. *Journal of Colloid and Interface Science.* **349:** 56-62.

Lordelo, M., Cid, J., Cordovil, C.M.D.S,, Alves. S.P., Bessa, R.J.B., Carolino, I. (2020). A comparison between the quality of eggs from indigenous chicken breeds and that from commercial layers. *Poultry Science.* **24:** 1768-1776. doi.org/10.1016/j.psj.2019.11.023.

Meskinfam, M., Bertoldi, S., Albanese, N., Cerri, A., Tanzi, M.C., Imani, R., Baheiraei, N., Farokhi, M. and Farè, S. (2018). Polyurethane foam/nano hydroxyapatite composite as a suitable scaffold for bone tissue regeneration. *Mater Sci. Eng C.* **82:** 130140. https://doi.org/10.1016/j.msec.2017.08.064.

Mondal, S., Park, S., Choi, J., Vu, T.T.H., Doan, V.H.M., Vo, T.T. *et al.* (2023). Hydroxyapatite: A journey from biomaterials to advanced functional materials. *Advances in Colloid and Interface Science.* **7:** 103013. doi.org/10.1016/j.cis.2023.103013.

Prabakaran, S., Rajan, M. (2021). The osteogenic and bacterial inhibition potential of natural and synthetic compound loaded metal-ceramic composite coated titanium implant for orthopedic applications. *New Journal of Chemistry.* **45:** 15996-16010.

Prakash, M., Rajan, H.K., Chandraprabha, M.N., Shetty, S., Mukherjee, T., Kumar, S.G. (2024). Recent developments in green synthesis of hydroxyapatite nanocomposites: Relevance to biomedical and environmental applications. *Green Chemistry Letters and Reviews.* **31:** 2422409. doi.org/10.1080/17518253.2024.2422409.

Rapacz-Kmita, A., Paluszkiewicz, C., Ślósarczyk, A., Paszkiewicz, Z. (2005). FTIR and XRD investigations on the thermal stability of hydroxyapatite during hot pressing and pressureless sintering processes. *Journal of Molecular Structure.* **744-747:** 653-656. doi.org/10.1016/j.molstruc.2004.11.070.

Ślósarczyk, A., Paszkiewicz Z., Paluszkiewicz, C. (2005). FTIR and XRD evaluation of carbonated hydroxyapatite powders synthesized by wet methods. *Journal of Molecular Structure.* **744-747:** 657-661.doi.org/10.1016/j.molstruc.2004.11.078.

Stipniece, L., Kondratjeva, A., Salma-Ancane, K. (2020). Influence of precursor characteristics on properties of porous calcium phosphate-titanium dioxide composite bioceramics. *Ceramics International.* **46:** 243-250.

Taz, M., Makkar, P., Imran, K.M., Jang, D.W., Kim, Y.S., Lee, B.T. (2019). Bone regeneration of multichannel biphasic calcium phosphate granules supplemented with hyaluronic acid. *Materials Science and Engineering C.* **15:** 1058-1066. doi.org/10.1016/j.msec.2019.02.051.

Vani, G., Veena, P., Kumar, R.V.S., Lashmi, M.S., Prameela, D.R., Kundu, B. (2021). Efficacy of multi-ion doped plasma spray Nano-hydroxyapatite coated titanium implants in long bone fracture repair in dogs- Radiographical and bone markers evaluation. *Indian Journal of Animal Research.* **56(3):** 348-352. doi.org/10.18805/ijar.b-4508.

Venkatesan, J., Jayakumar, R., Anil, S., Kim, S.k. (2016). Chitosan-nanohydroxyapatite Nanocomposite for Bone-tissue Regeneration. In: Elsevier eBooks. pp 161-174. doi.org/10.1016/b978-1-78242-452-9.00007-8.

Venkatesh, R., Ramanan, S.R. (2002). Influence of processing variables on the microstructure of sol-gel spun alumina fibres. *Materials Letters.* **1:** 189-195. doi.org/10.1016/s0167-577x(01)00644-9.